

# Conjugates of a Novel 7-Substituted Camptothecin with RGD-Peptides as $\alpha_v\beta_3$ Integrin Ligands: An Approach to Tumor-Targeted Therapy

Alma Dal Pozzo,<sup>\*,†</sup> Emiliano Esposito,<sup>†</sup> Minghong Ni,<sup>†</sup> Laura Muzi,<sup>†</sup> Claudio Pisano,<sup>‡</sup> Federica Bucci,<sup>‡</sup> Loredana Vesce,<sup>‡</sup> Massimo Castorina,<sup>‡</sup> and Sergio Penco<sup>‡</sup>

Istituto di Ricerche Chimiche e Biochimiche G. Ronzoni, via G. Colombo, 81, 20133, Milano, Italy, and Area of Oncology Research and Development, Sigma-Tau, Pomezia, Roma, Italy. Received February 24, 2010; Revised Manuscript Received September 30, 2010

Eight conjugates of a novel camptothecin derivative (Namitecan, NMT) with RGD peptides have been synthesized and biologically evaluated. This study focused on factors that optimize the drug linkage to the transport vector. The different linkages investigated consist of heterofunctional glycol fragments and a lysosomally cleavable peptide. The linkage length and conformation were systematically modified with the purpose to understand their effect on receptor affinity, systemic stability, cytotoxicity, and solubility of the corresponding conjugates. Among the new conjugates prepared, **C6** and **C7** showed high receptor affinity and tumor cell adhesion, acceptable stability in murine blood, and high cytotoxic activity ( $IC_{50} = 8$  nM). The rationale, synthetic strategy, and preliminary biological results will be presented.

## INTRODUCTION

The antitumor efficacy of clinically used anticancer drugs is limited by their nonspecific toxicity to normal cells, resulting in a low therapeutic index. Therefore, great efforts are being devoted to the aim of targeting therapeutics preferentially to tumors, sparing physiological tissues and decreasing side effects. In late years, several different approaches to this problem have been studied, which mainly focused on conjugating cytotoxic agents with macromolecules such as monoclonal antibodies (mAbs) or polymeric materials (1–5). First successes have been achieved with mAbs immunoconjugates, and some of them are currently in clinical trials. However, there are factors restricting the scope of this approach: the antigen-dependent drug delivery to target tumor cell population can be limited by the cell surface density of expressed antigens and by saturation of the receptors with immunoconjugates that are endocytosed at a given rate. The new generation immunoconjugates have incorporated drugs that are considerably more potent than the standard anticancer agents. Among them, the anti-CD33-calicheamicin (Mylotarg) has been approved by FDA for treatment of acute myeloid leukemia (6).

During the past two decades, the understanding of many receptors overexpressed by tumor cells during proliferation has given impetus to the development of low-molecular-weight selective ligands. Therefore, following a trend toward replacing the antibody scaffolds with small molecules, several peptides have been proposed as tumor-targeting tools, to be used as receptor imaging or as therapeutics when conjugated with antitumor agents; for recent reviews on this topic, see ref 7, 8. Small receptor-binding peptides offer the advantage of being easily synthesized, modified, and characterized in order to optimize their affinity to specific receptors.

Cyclic peptides containing the RGD (Arg-Gly-Asp) sequence are well-known as specific ligands of the  $\alpha_v\beta_3$  integrin cell

surface receptor. This integrin has a predominant role in tumor-induced angiogenesis and is overexpressed on the activated endothelial cells in several tumor forms, but expressed at a low level on normal and mature endothelial cells. Inhibition of angiogenesis has been shown to prevent tumor growth and even cause tumor regression in various experimental models (9). However, antiangiogenic therapy usually is not sufficient to eradicate tumors in the late stage. Thus, combination of antiangiogenic agents with either chemo or radiation therapy has demonstrated enhanced activity in multiple tumor systems (10). Ruoslathi et al. first raised the idea of conjugating a cytotoxic agent with RGD-containing peptides (11–13). Later on, many RGD peptides have been evaluated for their potential as antiangiogenic agents or integrin-targeted radiotracers and/or therapeutics (14–19).

We were interested in studying the effect of RGD cyclopeptides in conjugation with a new potent antitumoral drug belonging to the camptothecin family, Namitecan, NMT (20). A number of camptothecin prodrugs and delivery systems have been developed to improve the pharmacokinetic profile of this anticancer drug (21–23). We have previously reported on the synthesis and biological evaluation of a number of RGD–NMT conjugates (24), where the targeting RGD peptide was attached to the drug by either amide or hydrazone bond; in theory, both linkages should be potentially stable at physiological pH, whereas the main difference between them lies in the acid stability. During that study, we demonstrated that the amide bond-containing conjugates maintained good affinity to integrin receptors and accumulated in tumor cells after internalization, but showed no appreciable activity both in vitro and in vivo, indicating that the amide bond is too stable to promptly release the drug into the tumor cells. On the contrary, the hydrazone bond-containing conjugates exhibited high in vitro cytotoxicity, but their stability at pH 7.4 was much lower than expected; as a consequence, their activity has been mostly attributed to the NMT prematurely liberated within the cell culture medium. Thus, it was concluded that both types of linkage are not suitable for these low-molecular-weight conjugates. Moreover, all conjugates prepared were not soluble enough for a complete in vivo study, likely because the proximity of ligand and drug

\* To whom correspondence should be addressed. Dr. Alma Dal Pozzo, Ist. Di Ricerche Chimiche e Biochimiche G. Ronzoni, via Colombo 81, 20133 Milano, Italy. Tel.: +39-02-70600223; Fax: +39-02-70641634, e-mail: dalpozzo@ronzoni.it.

<sup>†</sup> Istituto di Ricerche Chimiche e Biochimiche G. Ronzoni.

<sup>‡</sup> Area of Oncology Research and Development.

Chart 1. Structure of NMT, Cyclopeptides P1 and P2, and Conjugates C1–C7

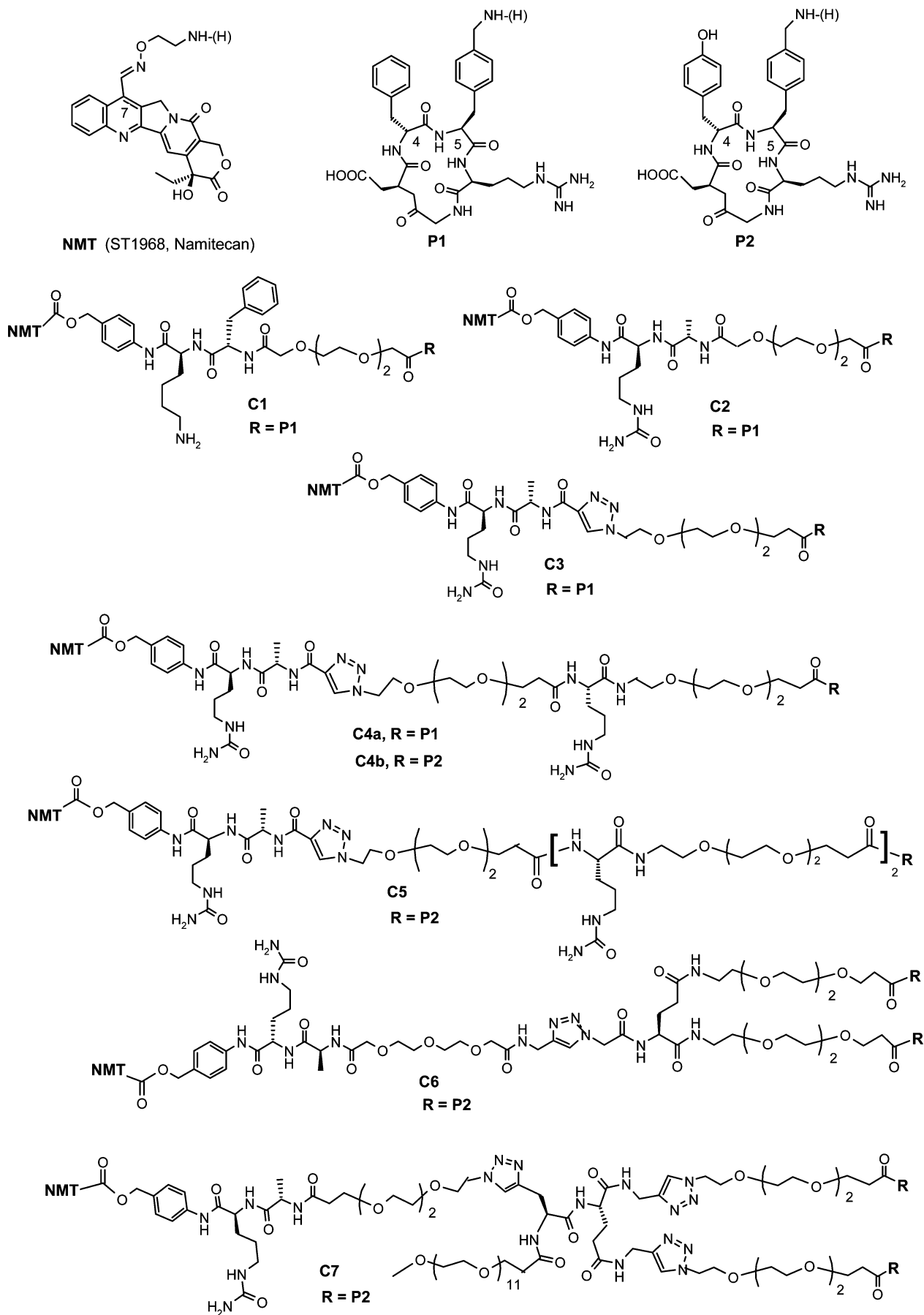
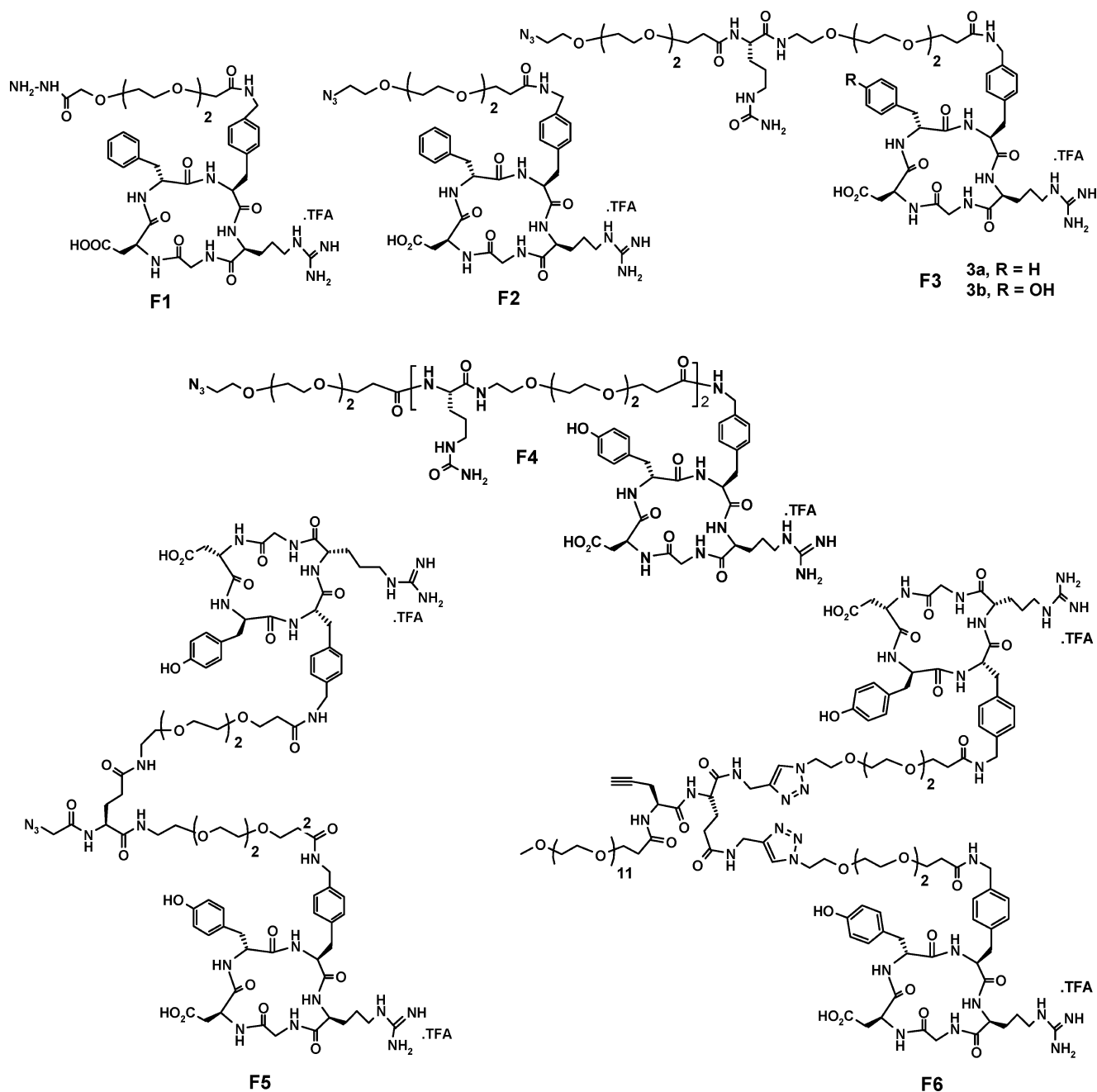


Chart 2. Structure of Fragments F1–F6, Containing Cyclopeptides



forms efficient intramolecular stacking interactions. Inspired by these results, we sought to verify another interesting approach, proposed in the literature and based on the introduction of selective protease-sensitive peptides into tumor-targeted conjugate spacers. These peptides have been claimed to be specific substrates of enzymes overexpressed within the lysosomal compartment of tumor cells, but rather stable to proteases in the systemic circulation (25–28).

Because of our interest in the potential of this approach, we have undertaken the development of a series of tumor-targeted conjugates containing an  $\alpha_v\beta_3$  integrin recognition moiety connected to NMT by different molecular bridges as spacers. The structure of these spacers include a peptide, that is enzymatically cleavable, but stable enough in the systemic circulation, and a number of glycol residues, whose length and conformation were systematically modified, in order to enhance solubility, without disturbing the binding of the RGD ligand to the receptor. The objective of the work described in this article

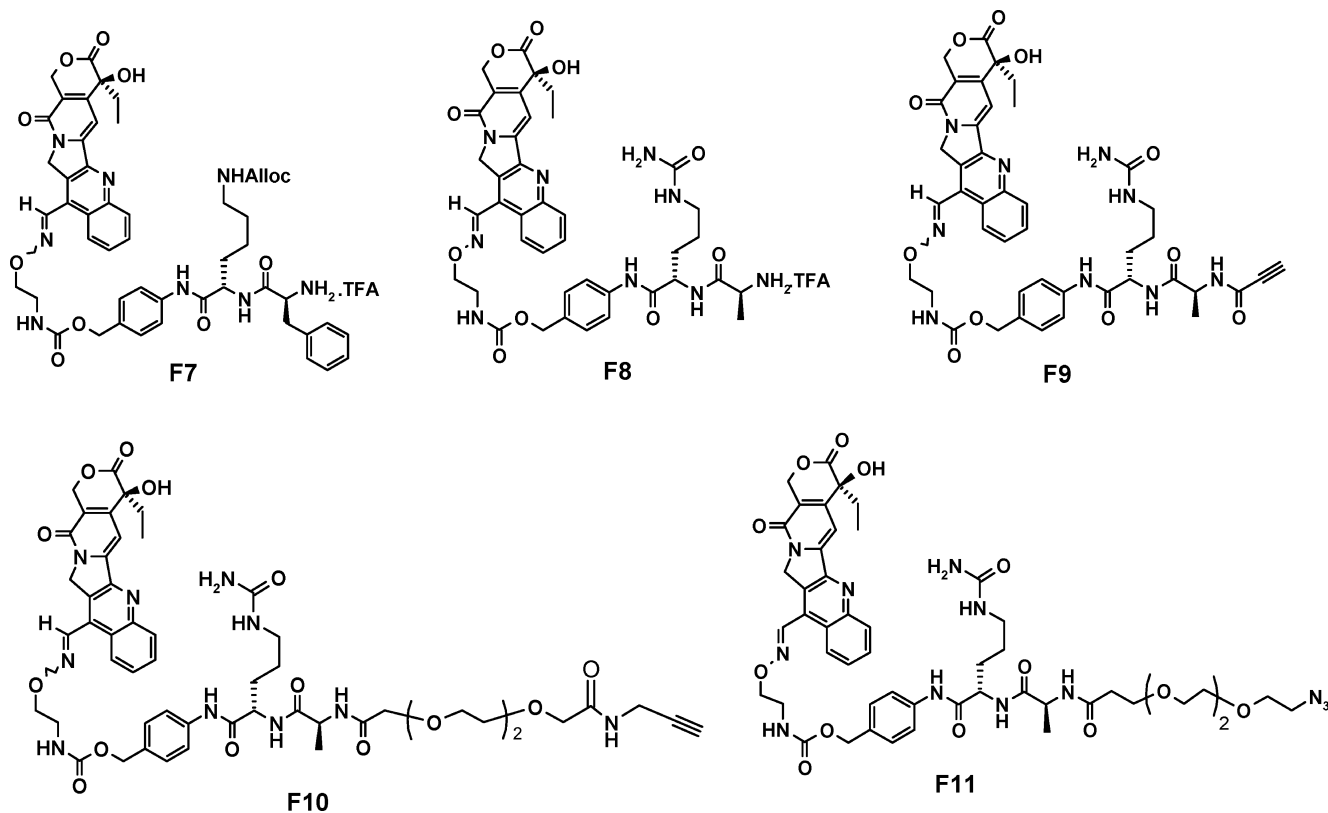
was to study the effect of the spacer modifications on receptor affinity, stability in murine blood, cytotoxicity, and solubility of the new conjugates.

Among a series of RGD cyclopeptide analogues of Cilengitide (29), designed and synthesized in our laboratories for the purpose of this study, we identified **P1** and **P2** to be used as targeting ligands, owing to their optimal stability and affinity to  $\alpha_v$  integrins (30). Peptide ligands, camptothecin derivative NMT, and conjugate structures are illustrated in Chart 1. The structure of the fragments used for assembling the conjugates is illustrated in Charts 2 and 3. Each pair of fragments, which were coupled together to obtain the desired conjugate, is described in Table 1.

## EXPERIMENTAL PROCEDURES

**Materials and Instruments.** All reagents and solvents were reagent grade and were distilled prior to use. All natural amino

Chart 3. Structure of Fragments F7–F11, Containing the Cytotoxic Drug NMT



acids and resin were purchased from Bachem (Switzerland). Fmoc-4-aminomethyl-phenylalanine (Amp) was purchased from PepTech Corporation, Burlington, MA, USA; the corresponding building blocks, Fmoc-Amp-glycol-R (where R can be amino, hydrazido, or azido group), were easily synthesized by standard methods. PEG derivatives were purchased from Iris Biotech GMBH (Germany). Namitecan (ST1968) was synthesized in Sigma-Tau laboratories (20). Microwave-assisted reactions were performed on a CEM MW instrument. Compounds were purified and characterized by a RP-HPLC 600 Waters instrument, equipped with a semipreparative column Alltima, Alltech, RP18, 10  $\mu$ , 22  $\times$  250 mm, or an analytical column Gemini, Phenomenex, C18, 5  $\mu$ , 4.6  $\times$  250 mm, at  $\lambda$  = 220 nm, using acetonitrile/water with 0.1% trifluoroacetic acid as mobile phase. <sup>1</sup>H NMR spectra were recorded on an AC300 Bruker instrument. Mass spectra were recorded on Bruker Autoflexaldi-Maldi-ToF or Micro-ToF Q instruments. Flash chromatography was carried out on silica gel Merck 230–400 mesh.

**Synthesis of Conjugate C1.** (Method A) As described in Scheme 1, fragment **F1** (350 mg, 0.319 mmol) and HOAT (259 mg, 1.91 mmol) were dissolved with 7 mL DMF; then, *t*-butyl nitrite (45  $\mu$ L, 0.383 mmol) was added and the mixture left under stirring at room temperature. After 30 min, 1 equiv of DIPEA was added, and the reaction mixture was poured into a solution containing fragment **F7** (337 mg, 0.319 mmol) in 2 mL DMF; pH was adjusted to 7.5 with DIPEA and the mixture left under stirring at room temperature, protected from light. After 2 h, an additional equivalent of the activated ester, prepared in situ as described above, was added, pH adjusted at 7.5, and left overnight. The solvent was removed at reduced pressure, and the residue was purified by preparative HPLC (40% CH<sub>3</sub>CN in H<sub>2</sub>O + 0.1% TFA). To remove the *N*-Alloc group, the compound was dissolved in 1 mL DMF, under argon, together with 2.5 mg of (Ph<sub>3</sub>P)<sub>4</sub>Pd, AcOH (12  $\mu$ L), and Bu<sub>3</sub>SnH (25  $\mu$ L), and stirred for 1 h. The final conjugate **C1** was obtained

after repeated precipitations with cool diethyl ether followed by lyophilization, with 97% purity.

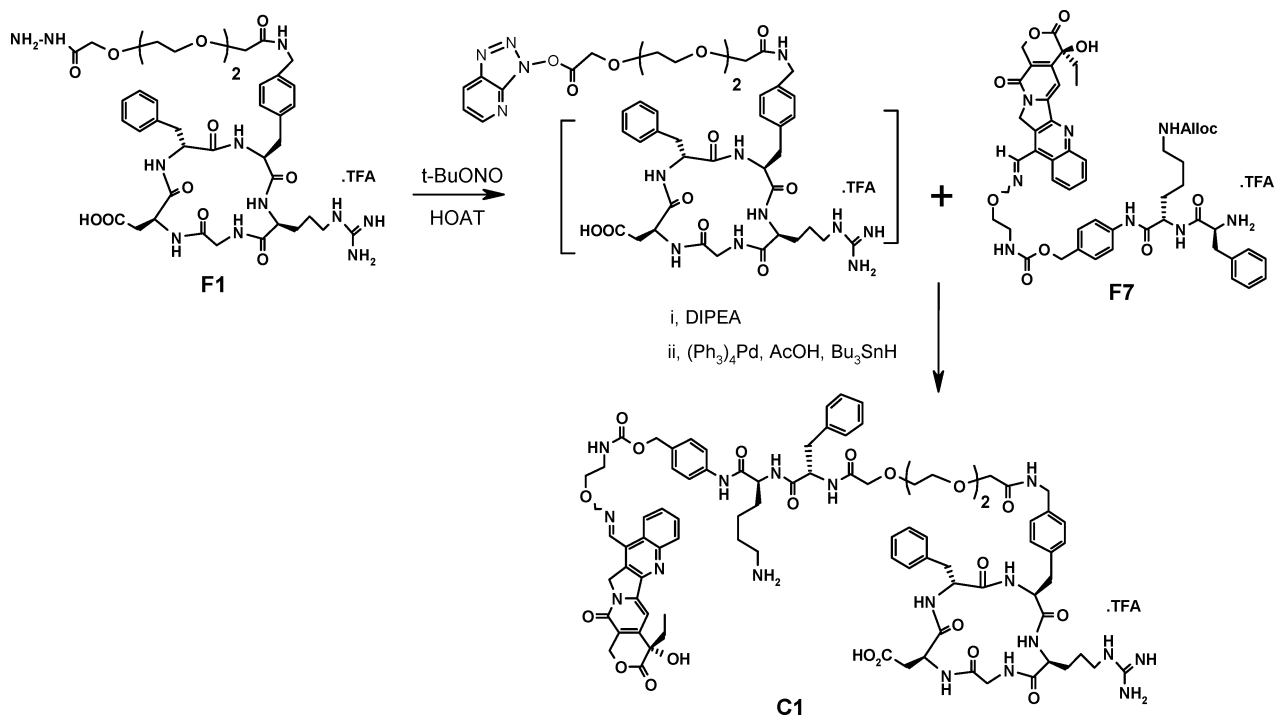
**Synthesis of Conjugate C2.** Coupling between fragments **F1** and **F8** was performed following the procedure described for conjugate **C1**. After purification by preparative HPLC and lyophilization, the compound was obtained with 97.6% purity.

**Synthesis of Conjugates C3–C7.** (Method B) General procedure. Two fragments, containing an alkyne and an alkylazido group, respectively, were assembled by Huisgen 1,3-dipolar cycloaddition. Equimolar amounts of the two desired fragments were dissolved in DMF. Aqueous solutions of sodium ascorbate (1 equiv) and CuSO<sub>4</sub>·5H<sub>2</sub>O (0.1 equiv) were added, pH was adjusted to 6 by addition of NaOH, and the suspension was stirred at room temperature overnight. When necessary to speed up the reaction, the mixture was submitted to microwave irradiation, 90 W for 2 min (*T*<sub>max</sub> obs 120 °C) once or twice until completion of the reaction, as monitored by HPLC. Final conjugates were obtained with >98% purity, after preparative HPLC and lyophilization.

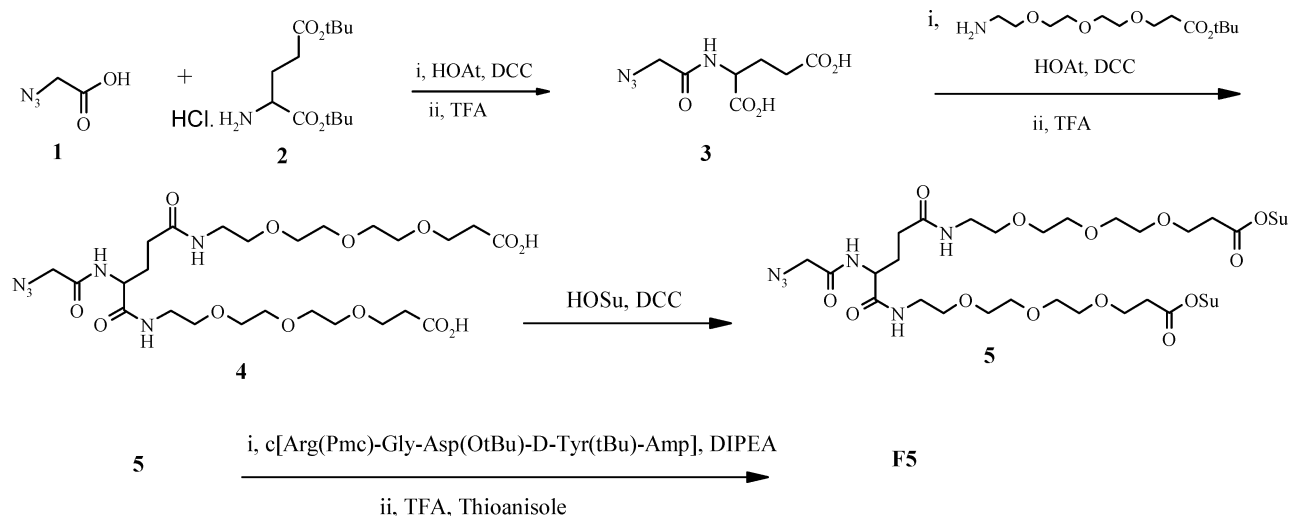
#### MW-Assisted Solid-Phase Synthesis of Cyclopeptides.

**General Procedure.** Solid-phase synthesis followed the standard Fmoc-protocol, starting from Fmoc-Gly-SASRIN. The amino acids (2 equiv) were added in the following order: Fmoc-Arg(Pmc)-OH, Fmoc-Amp(building block)-OH, Fmoc-D-Phe-OH (or Fmoc-D-Tyr(*t*Bu)-OH), and Fmoc-Asp(O*t*Bu)-OH. At each step, Fmoc deprotection was carried out with 20% piperidine. Energy applied: 30 W for 5 min (*t*<sub>max</sub> obs. 70 °C) for couplings and 25 W for 3 min (*t*<sub>max</sub> obs. 40 °C) for deprotections. For cleavage of the peptides, the resin was treated with 1% TFA in DCM during 15 min for 5 times and the filtrates immediately neutralized with pyridine. The collected filtrates were taken to dryness under vacuum, and the linear peptides were dissolved with acetonitrile containing 1% DIPEA to obtain a 1.5  $\times$  10<sup>-3</sup> M solution, then added with 3 equiv TBTU/HOBT and stirred for 1 h, until complete cyclization, as monitored by HPLC. After evaporation of the solvent, the cyclopeptides were

## Scheme 1. Synthesis of the Conjugate C1



## Scheme 2. Synthesis of Fragment F5

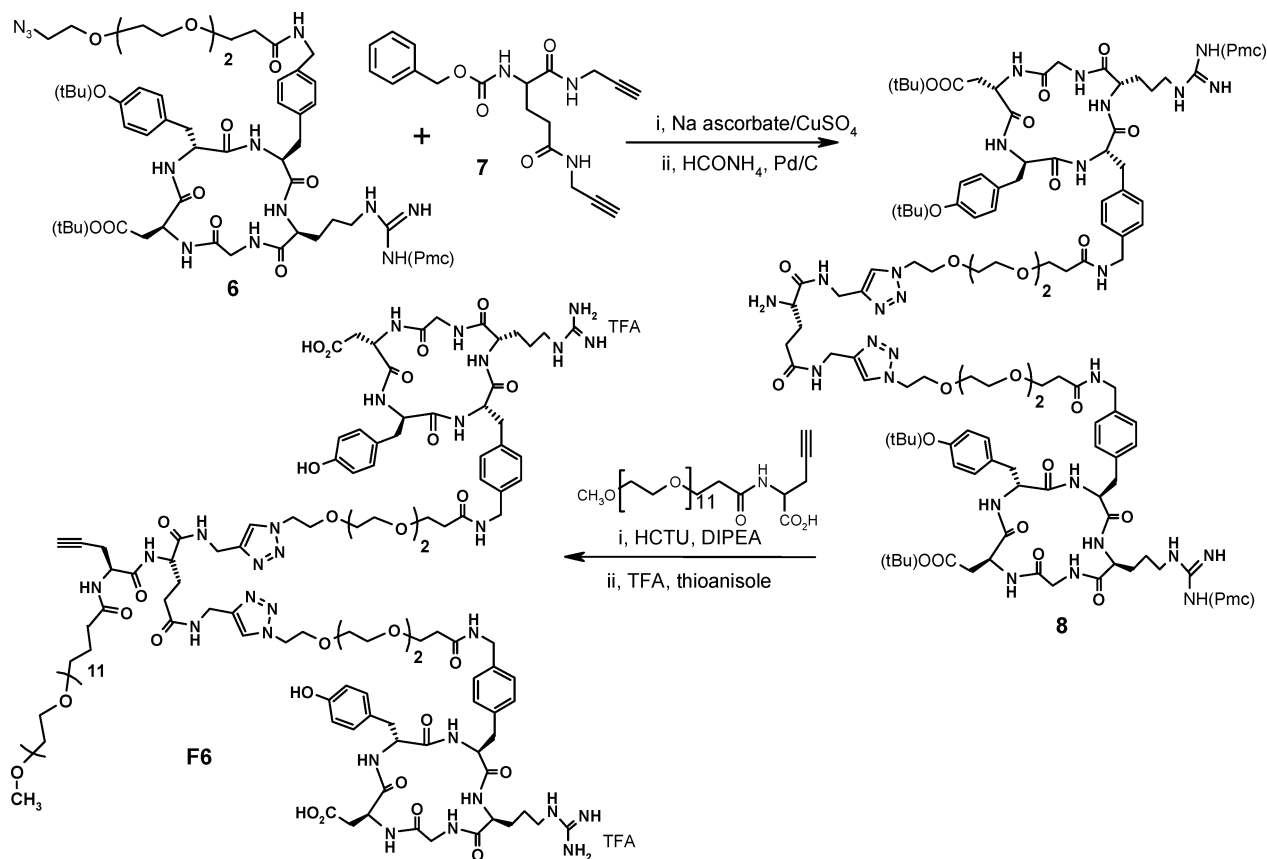


dissolved with DCM and washed (water, 0.1 N HCl, water). The organic phase, after drying with  $\text{Na}_2\text{SO}_4$ , was concentrated and the residue purified by flash chromatography (mobile phase, 95:5  $\rightarrow$  85:15 DCM/MeOH). Removal of the protecting groups was performed with 95:5 TFA/ $\text{H}_2\text{O}$  within 1 h. After concentration to small volume, the products were further purified by repeated precipitations with dry and cold diethyl ether. Total yields were around 50%, calculated on the amount of starting resin. The cyclopeptides prepared with this method differ from each other for the presence of D-Phe (**P1**) or D-Tyr (**P2**) at position 4 and for the Amp-building blocks at position 5.

**Synthesis of Fragment F5.** As described in the Scheme 2, DCC (84 mg, 0.405 mmol) was added to a cold solution of azidoacetic acid **1** (41 mg, 0.405 mmol), glutamic acid di-*tert*-butyl ester. HCl **2** (100 mg, 0.338 mmol), HOAT (0.405 mmol), and DIPEA (127 mL, 0.744 mmol) in 5 mL DCM. The reaction was stirred at room temperature for 2.5 h and after filtration was diluted up to 30 mL and washed with water, 0.1 N HCl, 5%  $\text{NaHCO}_3$ , and water. After removing the solvent, the residue

was treated with 3 mL of TFA for 1 h to afford 2-(2-azidoacetyl-amino)-pentanedioic acid **3**, which was dissolved with 45 mL of 8:1 DCM/DMF and coupled with *tert*-butyl 12-amino-4,7,10-trioxadodecanoate (281 mg, 1.01 mmol), HOAT (137 mg, 1.014 mmol), DIPEA (174 mL), and DCC (209 mg, 1.014 mmol) by the standard method to give a crude product that was purified by flash chromatography (95:5 DCM/MeOH) to obtain 175 mg of a solid white powder. Yield 68% (calc. for 3 steps). After deprotection with TFA, the bis-carboxylic intermediate **4** (0.234 mmol) was dissolved with 5 mL of DMF and treated with *N*-hydroxysuccinimide (108 mg, 0.936 mmol) and DCC (145 mg, 0.700 mmol) by stirring overnight. Solvent was removed and the succinimide **5**, dissolved with 8 mL DCM, was added to a solution of the partially protected cyclopeptide c[Arg(Pmc)-Gly-Asp(OtBu)-D-Tyr(tBu)-Amp], 728 mg, 0.66 mmol and DIPEA (113  $\mu\text{L}$ , 0.66 mmol) in 14 mL of DMF. After 1.5 h, solvent was removed and the residue purified by preparative HPLC (69%  $\text{CH}_3\text{CN}$ ). Yield 48%. Total deprotection was performed with 1:1 TFA/DCM containing 220 equiv of

## Scheme 3. Synthesis of Fragment F6



thioanisole. The pure fragment **F5** was obtained as a white solid after evaporation of the solvents and subsequent precipitations from cold diethyl ether. Yield 79%.

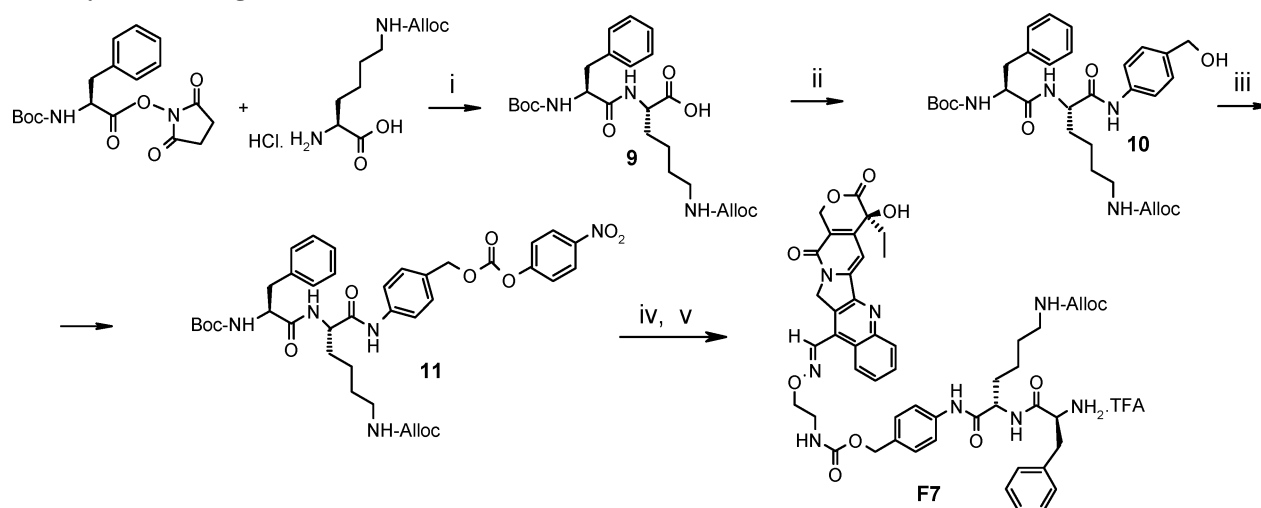
**Synthesis of Fragment F6.** As reported in Scheme 3, the totally protected cyclopeptide *c*{Arg(Pmc)-Gly-Asp(OtBu)-D-Tyr(OtBu)-Amp[CO-(CH<sub>2</sub>)<sub>2</sub>-(O-CH<sub>2</sub>-CH<sub>2</sub>)-O-(CH<sub>2</sub>)<sub>2</sub>-N<sub>3</sub>]} **6** (572 mg, 0.448 mmol) and 1,3-bis-(prop-2-ynylcarbamoyl-propyl)-carbamic acid benzyl ester **7** (72.5 mg, 0.206 mmol) were dissolved with 12 mL of 7:5 DMF/H<sub>2</sub>O. Then, 2.5 M sodium ascorbate (90  $\mu$ L) and 0.5 M CuSO<sub>4</sub>·5H<sub>2</sub>O (45  $\mu$ L) were added, and the mixture submitted to microwave irradiation (90 W, *T*<sub>max</sub> obs. 121 °C). The same operation was repeated three times until complete disappearance of the starting material, which was monitored by HPLC (35% CH<sub>3</sub>CN). After removing the solvent under reduced pressure, the crude residue was purified by flash chromatography (93:7 → 90:10 → 80:20 DCM/MeOH). Yield 71%. ESI mass: 1453.6 (*m/z* 2+), 969.4 (*m/z* 3+). 406 mg of this product was dissolved with 3:5 DMF/MeOH and orthogonally deprotected by means of ammonium formate (44 mg, 0.7 mmol) and Pd/C (200 mg). After 3 h stirring, the reaction was filtered, and the filtrate concentrated to give the intermediate **8**, which was dissolved with 3 mL DMF and used for the next step. *N*-(Methyl-PEG<sub>11</sub>-carboxy)-propargylglycine (102 mg, 0.149 mmol in 4.5 mL DCM) followed by HCTU (62 mg, 0.149 mmol) and DIPEA (51  $\mu$ L, 0.298 mmol) were added, and the resulting solution stirred for 2 h. After evaporation, the residue was redissolved with 300 mL of DCM and washed with water (2 × 50 mL). The organic phase was evaporated, and the fragment fully deprotected by means of a mixture of TFA/DCM/thioanisole (1:1:0.3). After taking to dryness, the residue was purified by repeated precipitations from TFA with cold diethyl ether, to afford 245 mg of fragment **F6**, with 41% yield (calculated from 3 steps).

**Conjugates Binding to  $\alpha_v\beta_3$  Integrin, Tumor Cell Adhesion, and in Vitro Cytotoxicity.** These assays were performed following the experimental procedures already published (24), and the results are reported in the Tables 5 and 7.

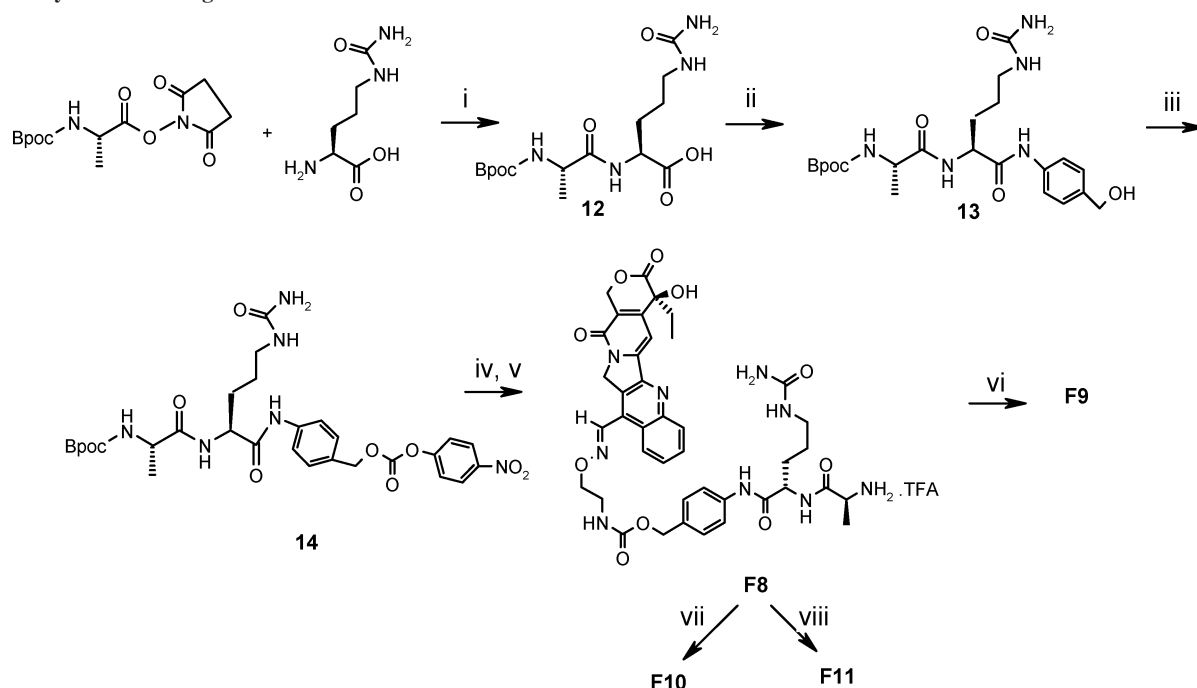
**Conjugate Stability in Murine Blood.** The blood of untreated healthy mice was collected in tubes containing 2% EDTA. The sample molecules were added to obtain a concentration of 5  $\mu$ M. The tubes were incubated at 37 °C under rotation for different sampling times during an interval of 3 h. At each time point, the samples were centrifuged at 1000g for 10 min, and the supernatants transferred in new tubes and stored at -20 °C. Plasma (100  $\mu$ L) was processed by adding 700  $\mu$ L of a cold mixture of 0.1% acetic acid and methanol (1:5 v/v). After vortexing, samples were kept at 20 °C for 10 min and then centrifuged at 14 000g for 10 min at 4 °C. The supernatants were analyzed by RP-HPLC-FL Beckman; column, Discovery HS-F5, 100 × 4.6 mm, 5  $\mu$ , Supelco; mobile phase, A = 0.1 M AcOH + 0.1% TEA, B = CH<sub>3</sub>CN; flow rate, 1 mL/min; spectrofluorometric detector, RF-10AXL Shimadzu; wavelengths,  $\lambda_{ex}$  370 nm and  $\lambda_{em}$  510 nm. A gradient elution was employed ranging from 25% to 33% B within 30 min. Data were acquired by computer system and processed by 32Karat Software, Beckman. Calibration curves were performed in plasma, and peak areas were used to calculate each calibration curve intercept and the slope of each calibration curve equation by weighted least-squares method, using *1/y* as weighting factor. All peaks were well-resolved from impurities of plasma and methods were linear in the tested range (*r*<sup>2</sup> > 0.985), with results suitable for quantification. Results are reported in Table 6 as a percentage of residual amounts found at each sampling time versus time zero (calculated using mean values of triplicate samples).

## RESULTS

**Synthesis.** Two groups of fragments have been prepared: the fragments **F1–F6** of the first group (Chart 2) contain one or

Scheme 4. Synthesis of Fragment F7<sup>a</sup>

<sup>a</sup> Reagents and conditions: (i) LiOH·H<sub>2</sub>O; (ii) 4-aminobenzylalcohol, HOAT, DCC; (iii) 4-nitrophenylchloroformate, py; (iv) 7-(2-aminoethoxyimino)-methyl-camptothecin.HCl, TEA, DMF; (v) TFA/DCM 1:1. Total yield 46.8%.

Scheme 5. Synthesis of Fragments F8–F11<sup>a</sup>

<sup>a</sup> Reagents and conditions: (i) LiOH·H<sub>2</sub>O; (ii) 4-aminobenzylalcohol, HOAT, DCC; (iii) 4-nitrophenylchloroformate, py; (iv) NMT, TEA; (v) 0.5% TFA in trifluoroethanol, 30 min, total yield 56.2%; (vi) propionic acid, HOAT, DCC; yield 72.6%; (vii) HCC-CH<sub>2</sub>-NH-CO-CH<sub>2</sub>-O-(CH<sub>2</sub>-CH<sub>2</sub>O)<sub>2</sub>-CH<sub>2</sub>-COOH, DCC, yield 63.5%; (viii) N<sub>3</sub>-(CH<sub>2</sub>)<sub>2</sub>-O-(CH<sub>2</sub>-CH<sub>2</sub>-O)<sub>2</sub>-(CH<sub>2</sub>)<sub>2</sub>-COOH, DCC, yield 62.8%.

two RGD cyclopeptides, which differ from each other for the amino acid in position 5 bearing glycol chains of different length and conformation. These fragments were built with good yields by MW-assisted SPPS, following cyclization in solution. In the case of the dimeric fragments **F5** and **F6**, two cyclopeptides were connected in solution through a dendron based on glutamic acid. The experimental procedures are given in detail and illustrated in Schemes 2 and 3. Fragments **F7–F11** of the second group (Chart 3) contain the camptothecin derivative and the lysosomally cleavable dipeptide. The dipeptide is connected to the *N*-terminal of the drug through 4-aminobenzylalcohol (PABA). PABA is a known self-immolative entity (31) that accomplishes a double function, to increase the distance between peptide and cytotoxic drug, allowing a better recognition by the endopeptidases, and to guarantee prompt release of

the parent drug through a 1,6-elimination mechanism, only after the enzymatic hydrolysis. The fragments belonging to the latter group were all prepared with similar synthetic procedures, except for minor modifications. In fact, during the synthesis of the first fragment **F7** (Scheme 4), deprotection of the terminal *N*-Boc caused a loss of about 10% of NMT, even reducing the TFA treatment to a few minutes. Therefore, *N*-Bpoc protection was used for fragments **F8–F11** (Scheme 5), because it can be removed with 0.5% TFA in trifluoroethanol without any cleavage of the carbamate bond.

In each fragment of both groups, a unique amino, hydrazido, azido, or alkyne function was introduced for further reaction with the corresponding counterpart to give the desired conjugates **C1–C7** (Chart 1). Each pair of fragments used for the synthesis of each conjugate is indicated in Table 1. The formation of

**Table 1. Reacting Fragments, Coupling Methods Used in the Synthesis of Conjugates C1–C7 and Yields**

fragments	conjugates	yields %
F1 + F7	C1 <sup>a</sup>	46.6
F1 + F8	C2 <sup>a</sup>	55.0
F2 + F9	C3 <sup>b</sup>	44.0
F3a + F9	C4a <sup>b</sup>	42.5
F3b + F9	C4b <sup>b</sup>	45.0
F4 + F9	C5 <sup>b</sup>	39.0
F5 + F10	C6 <sup>b</sup>	41.0
F6 + F11	C7 <sup>b</sup>	42.0

<sup>a</sup> Method A. <sup>b</sup> Method B.

conjugates needs a chemoselective synthesis. In fact, the reacting fragments must be used in a totally deprotected form, because the carbamate bond between NMT and the rest of the molecule is very sensitive to all late deprotection conditions. Two different methods were used: the conjugates C1 and C2 were synthesized via the acylazide method from the initial hydrazide, using the transfer active ester condensation

procedure (TAEC) introduced by Ramage et al. (32), as described in Scheme 1 (Method 1). Later on, for conjugates C3–C7, we found more convenient the use of Huisgen 1,3-dipolar reaction (33), (Method B). In fact, this cycloaddition affords cleaner products, because of its mild nature; moreover, grafting of the residual alkyne with the azide-terminated molecule enables the use of equivalent amounts of the two fragments, whereas the acylazide reaction requires two equivalents of the RGD counterpart. In the case of the bulkier conjugates, MW irradiation was applied to accelerate the reaction. Physico-chemical characterization of all fragments and conjugates is reported in the Tables 2, 3, and 4.

**Effect of Spacer on the Conjugate Receptor Affinity, Tumor Cell Adhesion, and Stability in Murine Blood.** The effects of spacer modifications on the behavior of the conjugates RGD–NMT are illustrated in Tables 5, 6, and 7. All spacers contain the dipeptide alanine-citrulline as a lysosomally cleavable sequence, except for C1, which contains phenylalanine-lysine. Within the series C2–C5, the spacers differ from each

**Table 2. Physico-Chemical Characterization of Conjugates C1–C7**

entry	HPLC <sup>c</sup> , rt, min <sup>b</sup>	Maldi mass [M+H] <sup>+</sup>	<sup>1</sup> H NMR
C1	9.0, 12.0 (35%)	1696.6	(DMSO- <i>d</i> <sub>6</sub> + D <sub>2</sub> O) δ 9.29 (s, 1H), 8.60 (d, 1H; <i>J</i> = 9.4), 8.22 (d, 1H, <i>J</i> = 9.4), 7.87 (t, 1H, <i>J</i> = 8.2), 7.73 (t, 1H, <i>J</i> = 8.2), 7.40 (s, 1H), 7.25 (d, 2H, <i>J</i> = 8.2), 7.20–7.10 (m, 14H), 7.03 (d, 2H; <i>J</i> = 8.2), 5.42–5.30 (m, 4H), 5.02 (s, 2H), 4.71–4.58 (m, 2H), 4.48–4.32 (m, 4H), 4.30–4.23 (m, 2H), 4.20–4.00 (m, 4H), 3.93 (s, 2H), 3.89–3.72 (m, 4H), 3.63–3.11 (m, 10H), 2.92–2.63 (m, 9H), 2.40–2.21 (m, 1H), 1.95–1.80 (m, 2H), 1.65–1.30 (m, 10H), 0.88 (t, 3H, <i>J</i> = 7.4).
C2	7.96, 10.4 (34%)	1650.71	(DMSO- <i>d</i> <sub>6</sub> + D <sub>2</sub> O) δ 9.29 (s, 1H), 8.60 (d, 1H, <i>J</i> = 9.4), 8.22 (d, 1H, <i>J</i> = 9.4), 7.87 (t, 1H, <i>J</i> = 8.2), 7.73 (t, 1H, <i>J</i> = 8.2), 7.36 (s, 1H), 7.24 (d, 2H, <i>J</i> = 8.5), 7.15–7.11 (m, 9H), 7.03 (d, 2H, <i>J</i> = 8.5), 5.42 (s, 2H), 5.36 (s, 2H), 4.95 (s, 2H), 4.64–4.60 (m, 1H), 4.45–4.27 (m, 8H), 4.07–4.00 (m, 3H), 3.94 (s, 2H), 3.90 (s, 2H), 3.59–3.46 (m, 10H), 3.09–2.66 (m, 9H), 2.40–2.33 (m, 1H), 1.90–1.86 (m, 2H), 1.75–1.38 (m, 8H), 1.24 (d, 3H, <i>J</i> = 6.9), 0.89 (t, 3H, <i>J</i> = 7.3).
C3	7.7, 9.9 (34%)	1745.7	(DMSO- <i>d</i> <sub>6</sub> + D <sub>2</sub> O) δ 9.19 (s, 1H), 8.50–8.40 (m, 2H), 8.19 (d, 1H, <i>J</i> = 8.4), 7.80 (t, 1H, <i>J</i> = 8.2), 7.74 (t, 1H, <i>J</i> = 8.2), 7.45 (d, 2H, <i>J</i> = 8.5), 7.39 (s, 1H), 7.19–6.95 (m, 11H), 5.48–5.30 (m, 3H), 5.19 (s, 1H), 4.89 (s, 2H), 4.69 (s, 1H), 4.60–4.24 (m, 8H), 4.20 (s, 2H), 4.13 (m, 1H), 4.02–3.98 (m, 2H), 3.89–3.75 (m, 2H), 3.52–3.37 (m, 10H), 3.30–3.22 (m, 2H), 3.10–2.62 (m, 9H), 2.40–2.30 (m, 3H), 1.91–1.81 (m, 2H), 1.76–1.38 (m, 8H), 1.34 (d, 3H, <i>J</i> = 6.9), 0.86 (t, 3H, <i>J</i> = 7.3).
C4a	11.2, 15.4 (30%)	2106.0	(DMSO- <i>d</i> <sub>6</sub> + D <sub>2</sub> O) δ 9.13 (s, 1H), 8.47–8.35 (m, 2H), 8.20–8.09 (m, 1H), 7.90–7.81 (m, 1H), 7.79–7.69 (m, 1H), 7.45–7.30 (m, 3H), 7.19–6.90 (m, 11H), 5.49–5.20 (m, 4H), 4.86 (s, 2H), 4.60–3.90 (m, 15H), 3.65–3.50 (m, 4H), 3.49–3.33 (m, 20H), 3.32–3.10 (m, 4H), 3.08–2.60 (m, 10H), 2.45–2.20 (m, 6H), 1.92–1.37 (m, 14H), 1.33 (d, 3H, <i>J</i> = 5.1), 0.85 (t, 3H, <i>J</i> = 5.7).
C4b	10.8, 15.2 (29%)	2120.89	(DMSO- <i>d</i> <sub>6</sub> ) δ 9.94 (s, 1H), 9.28 (s, 1H), 9.04 (s, 1H), 8.58 (d, 1H, <i>J</i> = 9.1), 8.52 (s, 1H), 8.30–8.16 (m, 3H), 8.15–7.98 (m, 2H), 7.97–7.72 (m, 5H), 7.62–7.48 (m, 3H), 7.37 (s, 1H), 7.25 (d, 2H, <i>J</i> = 8.5), 7.20–6.90 (m, 7H), 6.82 (d, 2H, <i>J</i> = 7.8), 6.56 (d, 2H, <i>J</i> = 7.6), 6.41 (s, 1H), 5.98–5.83 (m, 2H), 5.48–5.20 (m, 8H), 4.95 (s, 2H), 4.65–4.53 (m, 3H), 4.52–4.32 (m, 4H), 4.31–4.12 (m, 4H), 4.11–3.96 (m, 4H), 3.84 (t, 2H, <i>J</i> = 5.1), 3.65–3.35 (m, 24H), 3.20–2.80 (m, 16H), 2.45–2.33 (m, 4H), 1.98–1.83 (m, 2H), 1.82–1.40 (m, 12H), 1.35 (d, 3H, <i>J</i> = 7), 0.89 (t, 3H, <i>J</i> = 7.2).
C5	11.4, 16.2 (28%)	2480.0	(D <sub>2</sub> O) δ 8.73 (s, 1H), 8.52 (s, 1H), 7.83 (s, 1H), 7.75 (s, 1H), 7.62 (s, 1H), 7.39 (s, 1H), 7.19 (d, 2H, <i>J</i> = 7.9), 7.05 (d, 2H, <i>J</i> = 7.9), 7.00–6.80 (6H), 6.63 (d, 2H, <i>J</i> = 8.3), 5.65–5.40 (m, 4H), 5.05–4.85 (m, 2H), 4.70–4.62 (m, 2H), 4.60–4.25 (m, 14H), 4.10–4.00 (m, 2H), 3.95–3.35 (m, 34H), 3.30–3.10 (m, 10H), 3.00–2.50 (m, 16H), 2.15–2.05 (m, 2H), 2.00–1.45 (m, 17H), 1.15–1.05 (m, 3H).
C6	9.2, 12.6 (29%)	2988.78	(DMSO- <i>d</i> <sub>6</sub> + D <sub>2</sub> O) δ 9.30 (s, 1H), 8.57 (d, 1H, <i>J</i> = 8.2), 8.40 (s, 1H), 8.22 (d, 1H, <i>J</i> = 8.2), 7.91 (t, 1H, <i>J</i> = 7.1), 7.71 (t, 1H, <i>J</i> = 7.3), 7.52 (d, 2H, <i>J</i> = 8.5), 7.38 (s, 1H), 7.23 (d, 2H, <i>J</i> = 8.5), 7.18–7.04 (m, 8H), 6.81 (d, 4H, <i>J</i> = 8), 6.56 (d, 4H, <i>J</i> = 8.2), 5.42 (s, 2H), 5.38 (s, 2H), 5.22 (s, 1H), 5.10 (s, 2H), 4.93 (s, 1H), 4.74 (s, 1H), 4.38–4.34 (m, 9H), 4.26–4.14 (m, 7H), 4.06–4.03 (m, 2H), 3.90 (s, 4H), 3.91–3.83 (m, 2H), 3.62 (t, 4H, <i>J</i> = 6.1), 3.55–3.36 (m, 10H), 3.29–2.79 (m, 20H), 2.39 (t, 4H, <i>J</i> = 6.1), 2.20–2.08 (m, 2H), 1.89–1.82 (m, 3H), 1.75–1.33 (m, 13H), 1.23 (d, 3H, <i>J</i> = 6.9), 0.90–0.84 (m, 3H).
C7	10.0, 12.5 (29%)	3721.0	(DMSO- <i>d</i> <sub>6</sub> + D <sub>2</sub> O) δ 9.05 (s, 1H), 8.31 (d, 1H, <i>J</i> = 8.2), 8.10 (d, 1H, <i>J</i> = 8.2), 7.80 (t, 1H, <i>J</i> = 7.2), 7.77 (s, 1H), 7.73–7.61 (m, 3H), 7.40 (s, 1H), 7.43–7.29 (m, 2H), 7.06–6.99 (m, 10H), 6.80 (d, 4H, <i>J</i> = 8.2), 6.53 (d, 4H, <i>J</i> = 8.2), 5.49 (s, 2H), 5.43–5.11 (m, 4H), 4.79 (s, 1H), 4.57 (s, 1H), 4.43–4.11 (m, 24H), 3.70 (s, 6H), 3.60–3.30 (m, 78H), 3.17 (s, 3H), 3.05–2.70 (m, 20H), 2.40–2.22 (m, 10H), 2.20–1.23 (m, 16H), 1.19 (d, 3H, <i>J</i> = 7), 0.82 (t, 3H, <i>J</i> = 7).

<sup>a</sup> The conjugates show two peaks corresponding to *E/Z* isomers of the original cytotoxic molecule. <sup>b</sup> Acetonitrile % in the mobile phase is indicated in brackets.

**Table 3. Physico-Chemical Characterizations of Fragments F1–F6, Containing Cyclopeptide Residues**

entry	HPLC <sup>a</sup> , rt, min	Maldi mass [M + H] <sup>+</sup>	<sup>1</sup> H NMR
<b>F1</b>	9.14 (20%)	870.13	(DMSO- <i>d</i> <sub>6</sub> + D <sub>2</sub> O) δ 7.14–7.09 (m, 5H), 7.02–6.97 (m, 4H), 4.57–4.52 (m, 2H), 4.46–4.44 (m, 2H), 4.26 (s, 2H), 4.00 (d, 1H, <i>J</i> = 15), 3.95–3.90 (m, 2H), 3.57–3.51 (m, 8H), 3.26 (d, 1H, <i>J</i> = 15), 3.04 (t, 2H, <i>J</i> = 6.7), 2.87–2.64 (m, 5H), 2.38–2.33 (m, 1H), 1.75–1.72 (m, 1H), 1.51–1.47 (m, 1H), 1.34–1.32 (m, 2H).
<b>F2</b>	8.3 (30%)	881.0	(DMSO- <i>d</i> <sub>6</sub> + D <sub>2</sub> O) δ 7.13–6.98 (m, 9H), 4.57–4.52 (m, 1H), 4.47–4.40 (m, 1H), 4.31–4.28 (m, 1H), 4.27 (s, 2H), 4.03–3.98 (m, 2H), 3.62–3.48 (m, 12H), 3.32 (t, 2H, <i>J</i> = 5), 3.30 (d, 1H, <i>J</i> = 9), 3.04 (t, 2H, <i>J</i> = 6), 2.93–2.60 (m, 5H), 2.54–2.35 (m, 3H), 1.85–1.67 (m, 1H), 1.65–1.45 (m, 1H), 1.43–1.35 (m, 2H).
<b>F3a</b>	10.8 (25%)	1241.0	(D <sub>2</sub> O) δ 7.29–7.11 (m, 9H), 4.65 (t, 1H, <i>J</i> = 8.2), 4.40 (s, 2H), 4.35–4.17 (m, 4H), 3.76–3.56 (m, 24H), 3.49 (t, 2H, <i>J</i> = 4.7), 3.39–3.36 (m, 2H), 3.18–3.06 (m, 4H), 2.97–2.83 (m, 4H), 2.75–2.65 (m, 1H), 2.58 (t, 3H, <i>J</i> = 7.6), 1.85–1.34 (m, 8H).
<b>F3b</b>	8.9 (22%)	1256.96	(D <sub>2</sub> O) δ 7.43 (d, 2H, <i>J</i> = 8.2), 7.30 (d, 2H, <i>J</i> = 8.2), 7.18 (d, 2H, <i>J</i> = 8.8), 6.94 (d, 2H, <i>J</i> = 8.8), 4.93 (t, 1H, <i>J</i> = 6.5), 4.59 (s, 2H), 4.53–4.36 (m, 4H), 4.01–3.74 (m, 26H), 3.67 (t, 2H, <i>J</i> = 4.7), 3.59–3.52 (m, 2H), 3.35 (t, 2H, <i>J</i> = 7.0), 3.27 (t, 2H, <i>J</i> = 7.0), 3.14–3.04 (m, 5H), 2.95–2.87 (m, 1H), 2.79–2.72 (m, 4H), 2.03–1.58 (m, 8H).
<b>F4</b>	11.6 (21%)	1617.31	(D <sub>2</sub> O), δ 7.25 (d, 2H, <i>J</i> = 8.2), 7.12 (d, 2H, <i>J</i> = 8.2), 7.00 (d, 2H, <i>J</i> = 8.8), 6.76 (d, 2H, <i>J</i> = 8.8), 4.60 (t, 1H, <i>J</i> = 6.5), 4.42 (s, 2H), 4.31–4.19 (m, 6H), 3.83–3.57 (m, 40H), 3.52–3.40 (m, 5H), 3.36 (s, 4H), 3.21–3.07 (m, 6H), 2.96–2.67 (m, 2H), 2.62–2.51 (m, 6H), 1.92–1.30 (m, 12H).
<b>F5</b>	10.9 (22%)	1935.22	
<b>F6</b>	8.7 (26%)	2679.79	(DMSO- <i>d</i> <sub>6</sub> + D <sub>2</sub> O) δ 7.78 (s, 1H), 7.76 (s, 1H), 7.08 (d, 4H, <i>J</i> = 7.7), 7.01 (d, 4H, <i>J</i> = 8.2), 6.78 (d, 4H, <i>J</i> = 8.3), 6.54 (d, 4H, <i>J</i> = 8.2), 4.52–4.44 (m, 2H), 4.42–4.00 (m, 16H), 3.73 (t, 4H, <i>J</i> = 5.3), 3.60–3.54 (m, 7H), 3.50–3.37 (m, 67H), 3.31 (s, 1H), 3.26 (s, 1H), 3.20 (s, 3H), 3.02 (t, 5H, <i>J</i> = 6.5), 2.90–2.52 (m, 11H), 2.36 (t, 8H, <i>J</i> = 6.5), 2.19–2.10 (m, 2H), 2.0–1.90 (m, 1H), 1.80–1.68 (m, 4H), 1.55–1.42 (m, 2H), 1.35–1.28 (m, 4H)

<sup>a</sup> Acetonitrile % in the mobile phase is indicated in brackets.

**Table 4. Physico-Chemical Characterization of Fragments F7–F11, Containing the Cytotoxic Drug NMT**

entry	HPLC <sup>a</sup> , rt, min <sup>b</sup>	mass	<sup>1</sup> H NMR
<b>F7</b>	18.0, 25.0 (35%)	965.0 <sup>c</sup>	(DMSO- <i>d</i> <sub>6</sub> ) δ 9.96 (s, 1H), 9.28 (s, 1H), 8.56 (d, 1H, <i>J</i> = 8.5), 8.28 (s, 1H), 8.21 (d, 1H, <i>J</i> = 8.5), 8.05–8.00 (m, 1H), 7.90 (t, 1H, <i>J</i> = 7.4 Hz), 7.75 (t, 1H, <i>J</i> = 7.4), 7.52 (d, 1H, <i>J</i> = 8.4), 7.36 (s, 2H), 7.30–7.19 (m, 9H), 6.41 (s, 1H), 5.86–5.80 (m, 1H), 5.42–5.36 (m, 2H), 5.26–5.11 (m, 2H), 4.95 (s, 2H), 4.43–4.37 (m, 6H), 3.48 (t, 2H, <i>J</i> = 5.7), 3.00–2.61 (m, 4H), 1.90–1.82 (m, 2H), 1.74–1.50 (m, 2H), 1.49–1.35 (m, 2H), 1.30–1.18 (m, 2H), 0.82 (t, 3H, <i>J</i> = 7.2).
<b>F8</b>	12.0, 16.9 (26%)	812.32 <sup>d</sup>	(DMSO- <i>d</i> <sub>6</sub> ) δ 10.10 (s, 1H), 9.31 (s, 1H), 8.59 (d, 1H, <i>J</i> = 8.6), 8.22 (d, 1H, <i>J</i> = 8.5), 8.04 (s, 3H), 7.91 (t, 1H, <i>J</i> = 7.9), 7.76 (t, 1H, <i>J</i> = 8.1), 7.54 (d, 2H, <i>J</i> = 8.2), 7.36 (s, 1H), 7.25 (d, 2H, <i>J</i> = 8.6), 6.51 (s, 1H), 6.02 (t, 1H, <i>J</i> = 6.3), 5.45 (s, 2H), 5.42 (s, 2H), 5.36 (s, 2H), 4.95 (s, 2H), 4.50–4.47 (m, 1H), 4.37 (t, 2H, <i>J</i> = 5.6), 3.95–3.85 (m, 1H), 3.49–3.42 (m, 2H), 3.10–2.92 (m, 2H), 1.91–1.82 (m, 2H), 1.75–1.38 (m, 4H), 1.34 (d, 3H, <i>J</i> = 6.9), 0.88 (t, 3H, <i>J</i> = 7.2).
<b>F9</b>	11.4, 16.2 (31%)	885.8 <sup>c</sup>	
<b>F10</b>	11.6, 16.3 (32%)	1053.4 <sup>d</sup>	(DMSO- <i>d</i> <sub>6</sub> ) δ 9.89 (s, 1H), 9.28 (s, 1H), 8.58 (d, 1H, <i>J</i> = 8.2), 8.22 (d, 1H, <i>J</i> = 8.2), 8.11 (d, 1H, <i>J</i> = 7.8), 8.03–7.99 (m, 1H), 7.90 (t, 1H, <i>J</i> = 7.9), 7.76 (t, 1H, <i>J</i> = 7.9), 7.64 (d, 1H, <i>J</i> = 7.2), 7.55 (d, 2H, <i>J</i> = 8.4), 7.37 (s, 1H), 7.24 (d, 2H, <i>J</i> = 8.4), 6.41 (s, 1H), 5.91 (t, 1H, <i>J</i> = 5.7), 5.42 (s, 2H), 5.37 (s, 2H), 5.32 (s, 2H), 4.95 (s, 2H), 4.43–4.36 (m, 3H), 3.92 (s, 2H), 3.89 (s, 4H), 3.88–3.86 (m, 1H), 3.60–3.58 (m, 8H), 3.48–3.44 (m, 2H), 3.01–2.95 (m, 3H), 1.92–1.86 (m, 2H), 1.70–1.38 (m, 4H), 1.25 (d, 3H, <i>J</i> = 6.9), 0.89 (t, 3H, <i>J</i> = 7.3).
<b>F11</b>	9.0, 12.0 (36%)	1041.4 <sup>d</sup>	(DMSO- <i>d</i> <sub>6</sub> ) δ 9.81 (s, 1H), 9.28 (s, 1H), 8.51 (d, 1H, <i>J</i> = 9.0), 8.20 (d, 1H, <i>J</i> = 8.1), 7.89 (t, 1H, <i>J</i> = 7.1), 7.86–7.75 (m, 2H), 7.49 (d, 2H, <i>J</i> = 8.1), 7.39 (s, 1H), 7.21 (d, 2H, <i>J</i> = 8.4), 6.40 (s, 1H), 5.90–5.88 (m, 1H), 5.42 (s, 2H), 5.37 (s, 2H), 5.31 (s, 2H), 4.95 (s, 2H), 4.39–4.27 (m, 4H), 3.60–3.49 (m, 14H), 3.37 (t, 2H, <i>J</i> = 4.8), 3.01–2.95 (m, 2H), 2.40–2.38 (m, 2H), 1.90–1.86 (m, 2H), 1.71–1.38 (m, 4H), 1.20 (d, 3H, <i>J</i> = 7.0), 0.89 (t, 3H, <i>J</i> = 7.2).

<sup>a</sup> Acetonitrile % in the mobile phase is indicated in brackets. <sup>b</sup> These fragments show two peaks corresponding to *E/Z* isomers of the original cytotoxic molecule. <sup>c</sup> Maldi [M + Na]<sup>+</sup>. <sup>d</sup> Esi [M + H]<sup>+</sup>.

other for the length and disposition of the hydrophilic glycol chains, whereas the spacers of conjugates **C6** and **C7** contain two RGD ligands connected to the drug through multiple glycol chains in a branched conformation. In Table 5, the conjugate affinity to α<sub>v</sub>β<sub>3</sub> integrin and their tumor cell adhesion is reported in parallel with the ligand cyclopeptides and the drug alone. **C1–C3**, bearing a short glycol between ligand and drug, showed very poor solubility and lost affinity to the receptor if compared with the ligand alone, most probably due to steric hindrance induced by the drug. However, when the glycol spacers were elongated in **C4–C5**, affinity and solubility improved, but the stability decreased, as it is possible to observe in Table 6. This is consistent with the results reported in Table 7: as stability

decreased, cytotoxicity increased, obviously due to some amounts of the free drug in the culture media. Only the dimeric conjugates **C6** and **C7** exhibited good receptor affinity and cytotoxicity, together with sufficient stability and optimal solubility.

Cell adhesion of the conjugates resulted generally increased with respect to RGD peptides alone, and this may be attributed to cooperative adhesion of the whole molecule.

## DISCUSSION

In the present work, RGD peptides as targeting moieties were conjugated to the cytotoxic agent Namitecan through

**Table 5. Binding to Isolated  $\alpha_v\beta_3$  Integrin<sup>a</sup> of Conjugates C1–C7 and Their Effect on Adhesion to PC3 (Prostatic Carcinoma) and A2780 (Ovarian Carcinoma) Cell Lines, in the Presence of Vitronectin, after 3 h Treatment**

entry	binding, IC <sub>50</sub> nM		cell adhesion, IC <sub>50</sub> $\mu$ M	
	$\alpha_v\beta_3$		PC3	A2780
<b>P1</b>	1.70 $\pm$ 0.10		23.20 $\pm$ 5.02	3.80 $\pm$ 0.30
<b>P2</b>	1.08 $\pm$ 0.12		25.20 $\pm$ 4.50	4.50 $\pm$ 0.20
<b>C1</b>	9.71 $\pm$ 0.06		1.80 $\pm$ 0.40	2.70 $\pm$ 0.30
<b>C2</b>	30.40 $\pm$ 2.25		2.10 $\pm$ 0.20	0.90 $\pm$ 0.05
<b>C3</b>	11.00 $\pm$ 0.81		0.56 $\pm$ 0.07	0.67 $\pm$ 0.02
<b>C4a</b>	2.99 $\pm$ 0.26		1.60 $\pm$ 0.80	1.70 $\pm$ 0.20
<b>C4b</b>	4.36 $\pm$ 0.22		0.50 $\pm$ 0.09	1.70 $\pm$ 0.10
<b>C5</b>	9.38 $\pm$ 0.17		1.40 $\pm$ 0.20	5.40 $\pm$ 0.30
<b>C6</b>	3.00 $\pm$ 0.10		0.39 $\pm$ 0.09	0.45 $\pm$ 0.02
<b>C7</b>	6.20 $\pm$ 0.08		1.00 $\pm$ 0.05	1.00 $\pm$ 0.00
<b>NMT</b>	no binding		no adhesion	

<sup>a</sup> Nonspecific binding was determined in the presence of 1  $\mu$ M Echistatin.

**Table 6. Stability of Conjugates C1–C7 in the Whole Blood of CD1 Mice, Expressed as Percentage of Residual Amounts Found at Different Hours vs Time Zero**

entry	1 h	2 h	3 h
<b>C1</b>	1.8	n.d.	n.d.
<b>C2</b>	100	100	100
<b>C3</b>	56	34	20
<b>C4a</b>	34	8	0.9
<b>C4b</b>	35	9	1.5
<b>C5</b>	38	11	2.5
<b>C6</b>	76	73	67
<b>C7</b>	67	61	51

**Table 7. Cytotoxicity of Conjugates C1–C7, after 3 h Treatment, IC<sub>50</sub>  $\mu$ M**

entry	PC3	A2780
<b>C1</b>	0.22 $\pm$ 0.003	0.0084 $\pm$ 0.0006
<b>C2</b>	4.60 $\pm$ 0.80	0.095 $\pm$ 0.02
<b>C3</b>	1.00 $\pm$ 0.10	0.03 $\pm$ 0.003
<b>C4a</b>	2.50 $\pm$ 0.70	0.009 $\pm$ 0.0007
<b>C4b</b>	0.84 $\pm$ 0.20	0.013 $\pm$ 0.0006
<b>C5</b>	0.42 $\pm$ 0.05	0.02 $\pm$ 0.003
<b>C6</b>	1.00 $\pm$ 0.02	0.008 $\pm$ 0.0005
<b>C7</b>	1.00 $\pm$ 0.01	0.008 $\pm$ 0.0001
<b>NMT</b>	0.36 $\pm$ 0.05	0.0049 $\pm$ 0.0003
<b>P1</b>	>3000	>3000
<b>P2</b>	>3000	>3000

different spacers, consisting of linear or branched glycol residues and a peptide suitable for releasing the drug by enzymatic hydrolysis inside the tumor cell. The products were evaluated for their in vitro tumor cell-targeting efficacy, stability in murine blood, solubility, and cytotoxicity, with the purpose of studying their structure–activity relationship. Since the spacers between carrier and drug play the main role in the fate of small targeted drug conjugates, we systematically modified these molecular bridges in a continuing effort to reach a fine balance between sufficient systemic stability and cleavability inside the tumor cells, while preserving high receptor affinity and solubility of the whole conjugate. In the first conjugate **C1**, a spacer containing the Phe-Lys dipeptide was introduced, because this sequence had been proposed by Dubowchick et al. (26, 27) for rapid lysosomal hydrolysis and high human plasma stability. However, we assisted at the total cleavage of **C1** within one hour in the murine blood. In a search for more stable peptides, we evaluated other peptide sequences (such as D-Ala-Phe-Lys, Val-Cit, Aib-Cit, Tic-Cit), but with negative results (Dal Pozzo, A., Ni, M., and Bucci, F. Data not published. We also confirmed with our representative examples that compounds lacking the PABC self-immolative group do not

release CPT, probably because of the steric crowding of the bulky drug), even though some of them have been used with success in the literature, mainly for immunoconjugates. Finally, the Ala-Cit dipeptide was found to have a significantly longer life in murine blood, together with sufficient cleavability by tumor cell associated proteases, as demonstrated by the cytotoxic activity of the corresponding conjugates; thus, Ala-Cit was adopted in all subsequent conjugate spacers. However, the stability was greatly influenced by the rest of the molecule, and this is observable with conjugates **C3**–**C5**, where elongation of the hydrophilic glycol chains led to a decrease of the half-life in the murine blood (see Table 6). To improve the solubility, we chose to substitute the commonly used large poly(ethylene glycol)s (PEGs) with a number of small glycol chains. In fact, PEGs, which are unique water-solubilizing agents currently employed for bioactive systems, are commercially available as polydisperse oligomers, and would yield undesirable heterogeneous products; moreover, because of their conformational flexibility, they tend to create bulky loops that can interfere with the ligand binding to the receptor. On the contrary, short glycols can be distributed on strategic positions of the molecular construct with respect to both the targeting and cleavable peptides. At first, we introduced in the spacers short glycol fragments connected in series through citrulline residues, which, beyond increasing hydrophilicity, should impart rigidity to the chain by their amide bonds, without shielding the ligand from recognition. Nevertheless, this strategy proved unsuccessful: in fact, as solubility improved, stability decreased, and cytotoxicity increased, due to the presence of significant amounts of the parent drug. This behavior indicates that the cleavable peptide is more exposed to the blood proteases. A deshielding effect is also observable in the conjugate **C3**, where the rigid triazole linkage orients the spacer chain away from the cleavable dipeptide moiety, where it is more accessible. On the other hand, solubility issues are a potentially negative aspect that could be a serious obstacle for preclinical development, and introduction of hydrophilic moieties is unavoidable. In an attempt to increase pegylation, while maintaining plasma stability and affinity to the receptor, we designed dimeric conjugates containing two RGD linked to a dendron unit bearing different glycol chains, to obtain a multifunctional platform where different pendant domains can be strategically allocated, without disturbing each other. Moreover, this approach exploits the multivalency effect on the ligand affinity (16, 18, 34). In this way, we could find conjugates **C6** and **C7**, endowed with the desired characteristics (increased avidity for the receptor together with appreciable stability and solubility), which demonstrated superior in vitro efficacy.

## CONCLUSION

Our study highlights the crucial role of the spacer between targeting device and drug in tumor-targeted conjugates. Unlike immunoconjugates (where the bulky nature of the targeting molecule is less sensitive to the influence of the drug and spacer counterparts, and can shield and stabilize the connecting bond from premature hydrolysis), engineering conjugates with low-molecular-weight ligands is a most challenging problem, its success depending on a plateau of different factors. In fact, the small targeting molecule must retain tumor binding after substitution with molecules, that may be of similar or larger size, and the addition of new domains results in the modification of existing domains affecting their properties. Accordingly, careful selection of the enzymatically cleavable peptide and the length and disposition of the hydrophilic chains should be necessary for

the development of each single small targeting molecule for therapeutic application, since the strategy is not generalizable. We tried to help bring order to this sometimes unruly subject, and optimized the properties of our conjugates after a systematic *in vitro* study. Our results demonstrate the potential of tumor-targeted delivery of conjugates based on the specific recognition of the integrin RGD ligands and selective release of the drug by tumor-associated enzymes. However, we are aware of possible *in vivo* problems, such as the following: (1) Partial distribution of free drug generated through extracellular proteases cannot be ruled out. (2) The hydrophilic compounds synthesized may undergo rapid renal clearance, and larger PEGs would be needed to enhance the retention time in the circulation and allow proper tumor accumulation. Nevertheless, an improved therapeutic index could be expected by tumor specific delivery of at least a part of the targeted drug, resulting in lower and therefore less toxic systemic doses necessary to obtain the antitumor effect. Further evaluation of conjugates C6 and C7 in preclinical animal models for tumor growth inhibition and acute toxicity studies are currently in progress.

#### ACKNOWLEDGMENT

We are grateful to Sigma-Tau, Roma, Italy, for financial assistance. We thank Gianni Dottori for technical assistance.

#### LITERATURE CITED

- (1) Doronina, S. O., Toki, B. E., Torgov, M. Y., Mendelsohn, B. A., Cerveny, C. G., Chace, D. F., DeBlank, R. I., Gearing, R. P., Bovee, T. D., Siegall, C. B., Francisco, J. A., Wahl, A. F., Meyer, D. I., and Senter, P. D. (2003) Development of potent monoclonal antibody auristatin conjugates for cancer therapy. *Nat. Biotechnol.* *21*, 778–784.
- (2) Jaracz, S., Chen, J., Kuznetsova, L. V., and Ojima, I. (2005) Recent advances in tumor-targeting drug conjugates. *Biorg. Med. Chem.* *13*, 5043–5054.
- (3) Temming, K., Meyer, D. L., Zabinski, R., Dijkers, E. C. F., Poelstra, K., Molema, G., and Kok, R. J. (2006) Evaluation of RGD-targeted albumin carriers for specific delivery of auristatin E to tumor blood vessels. *Bioconjugate Chem.* *17*, 1385–1394.
- (4) Chari, R. V. J. (2008) Targeted cancer therapy: conferring specificity to cytotoxic drugs. *Acc. Chem. Res.* *41*, 98–107.
- (5) Ducry, L., and Stump, B. (2010) Antibody-drug conjugates: linking cytotoxic payloads to monoclonal antibodies. *Bioconjugate Chem.* *21*, 5–13.
- (6) Hamman, P. R., Hinman, L. M., Hollander, I., Beyer, C. F., Lindh, D., Holcomb, R., Hallett, W., Tsou, H. R., Upešlacis, J., Shochat, D., Mountain, A., Flowers, D. A., and Bernstein, I. (2002) Gentuzumab ozogamicin: a potent and selective anti-CD33 antibody-calicheamicin conjugate for treatment of acute myeloid leukemia. *Bioconjugate Chem.* *13*, 47–58.
- (7) Okarvi, S. M. (2004) Peptide-based radiopharmaceutical; future tools for diagnostic imaging of cancer and other diseases. *Med. Res. Rev.* *24*, 357–397.
- (8) Zaccaro, L., del Gatto, A., Pedone, C., and Saviano, M. (2009) Peptides for tumor therapy and diagnosis: current status and future directions. *Curr. Med. Chem.* *16*, 780–795.
- (9) Cristofanilli, M., Charnsangavej, C., and Hortobagyi, G. N. (2002) Angiogenesis modulation in cancer research: novel clinical approaches. *Nat. Rev. Drug Discovery* *1*, 415–426.
- (10) Jain, R. K. (2003) Molecular regulation of vessel maturation. *Nat. Med.* *9*, 685–693.
- (11) Ruoslati, E., and Pierschbacher, M. D. (1987) New perspective in cell adhesion RGD and integrins. *Science* *238*, 491–497.
- (12) Pasqualini, R., Koivunen, E., and Ruoslati, E. (1997)  $\alpha_v$  integrins as receptors for tumor targeting by circulating ligands. *Nat. Biotechnol.* *15*, 542–546.
- (13) Arap, W., Pasqualini, R., and Ruoslati, E. (1998) Cancer treatment by targeted drug delivery to tumor vasculature in a mouse model. *Science* *279*, 377–380.
- (14) Haubner, R., and Wester, H. J. (2004) Radiolabelled tracers for imaging of tumor angiogenesis and evaluation of antiangiogenic therapies. *Curr. Pharm. Des.* *10*, 1439–455.
- (15) Temming, K., Schiffelers, R. M., Molema, G., and Kok, R. J. (2005) RGD-based strategies for selective delivery of therapeutics and imaging agents to the tumor vasculature. *Drug Resistance Updates* *8*, 381–402.
- (16) Chen, X., Plasencia, C., Hou, Y., and Neamati, N. (2005) Synthesis and biological evaluation of dimeric RGD peptide-placlitaxel conjugate as a model for integrin-targeted drug delivery. *J. Med. Chem.* *48*, 1098–1106.
- (17) Meyer, A., Auernheimer, J., Modlinger, A., and Kessler, H. (2006) Targeting RGD recognizing integrins: drug development, biomaterial research, tumor imaging and targeting. *Curr. Pharm. Des.* *12*, 2723–2747.
- (18) Rypka, C., Mann-Steinberg, H., Fichtner, I., Weber, H., Satchi-Fainaro, R., Binossek, M. L., and Kratz, F. (2008) *In vitro* and *in vivo* evaluation of doxorubicin conjugates with the divalent peptide E-[c(RGDfK)<sub>2</sub>] that targets integrin  $\alpha_v\beta_3$ . *Bioconjugate Chem.* *19*, 1414–422.
- (19) McNerny, A. M., Kukowska-Latallo, J. F., Mullen, D. G., Wallace, J. M., Desai, A. M., Shukla, R., Huang, B., Holl, M. M. B., and Baker, J. R. (2009) RGD dendron bodies: synthetic avidity agents with defined and potentially interchangeable effector sites that can substitute for antibodies. *Bioconjugate Chem.* *20*, 1853–1859.
- (20) Pisano, C., De Cesare, M., Beretta, G. L., Zuco, V., Pratesi, G., Penco, S., Vesce, L., Foderà, R., Ferrara, F. F., Guglielmi, M. B., Carminati, P., Dalla valle, S., Morini, G., Merlini, L., Orlandi, A., and Zumino, F. (2008) Preclinical profile of antitumor activity of a novel Hydrophilic camptothecin, ST1968. *Mol. Cancer Ther.* *7*, 2051–2059.
- (21) Conover, C. D., Greenwald, R. B., Pendri, A., Gilbert, K. W., and Shum, K. L. (1998) Camptothecin delivery systems. Enhanced efficacy and tumor accumulation of camptothecin following its conjugation to poly(ethylene glycol) via a glycine linker. *Cancer Chemother. Pharmacol.* *42*, 407–414.
- (22) Caiolfa, V. R., Zamai, M., Fiorino, A., Frigerio, E., Pellizzoni, C., d'Argi, R., Ghiglieri, A., Castelli, M. G., Farao, M., Pesenti, E., Gigli, M., Angelucci, F., and Suarato, A. (2000) Polymer-bound camptothecin: initial biodistribution and antitumor activity studies. *J. Controlled Release* *65*, 105–119.
- (23) Lerchen, H. G., Baumgarten, J., von dem Bruch, K., Lehmann, T. E., Sperzel, M., Kempka, G., and Fiebig, H. H. (2001) Design and optimization of 20-O-linked camptothecin glycoconjugates as anticancer agents. *J. Med. Chem.* *44*, 4186–4195.
- (24) Dal Pozzo, A., Ni, M. H., Esposito, E., Dallavalle, S., Musso, L., Bargiotti, A., Pisano, C., Vesce, L., Bucci, F., Castorina, M., Foderà, R., Giannini, G., and Penco, S. (2010) Novel tumor-targeted RGD peptide-camptothecin conjugates: synthesis and biological evaluation. *Biorg. Med. Chem.* *18*, 64–72.
- (25) Duncan, R., Cable, H. C., Lloyd, J. B., Rejmanova, P., and Kopecek, J. (1983) Polymers containing enzymatically degradable bond. 7. Design of oligopeptides side chains in poly N-2-hydroxypropylmethacrylamide copolymers to promote degradation by lysosomal enzymes. *Macromol. Chem.* *184*, 1997–2008.
- (26) Dubowchik, G. M., and Firestone, R. A. (1998) Cathepsin B-sensitive dipeptide prodrugs. I. A model study of structural requirements for efficient release of Doxorubicin. *Biorg. Med. Chem. Lett.* *8*, 3341–3346.
- (27) Dubowchik, G. M., Firestone, R. A., Padilla, L., Willner, D., Hofstead, S. J., Mosure, K., Knipe, J. O., Lash, S. J., and Trail, P. A. (2002) Cathepsin B-labile dipeptide linkers for lysosomal release of doxorubicin from internalizing immunoconjugates: model studies of enzymatic drug release and antigen-specific *in vitro* antitumor activity. *Bioconjugate Chem.* *13*, 858–869.

- (28) Shiose, Y., Kuga, H., Ohki, H., Ikeda, M., Yamashita, F., and Hashida, M. (2009) Systematic research of peptide spacers controlling drug release from macromolecular prodrugs system, carboxymethyl-dextran-polyalcohol-peptide drug conjugates. *Bioconjugate Chem.* 20, 60–70.
- (29) Haubner, R., Finsinger, D., and Kessler, H. (1997) Stereoisomeric peptide libraries and peptidomimetics for designing selective inhibitors of the  $\alpha_v\beta_3$  integrin for a new cancer therapy. *Angew. Chem.* 36, 1374–1389.
- (30) Dal Pozzo, A., Penco, S., Giannini, G., Tinti, O., Pisano, C., Vesci, and L., Ni, M. H. Cyclopeptide derivatives with anti-integrin activity, EP 1 751 176 B1, October 3, 2010.
- (31) Carl, P. L., Chakravarty, P. K., and Katzenellenbogen, J. A. (1980) A novel connector linkage applicable in prodrug design. *J. Med. Chem.* 24, 479–480.
- (32) Wang, P., Layfield, R., Landon, M., Mayer, R. J., and Ramage, R. (1998) Transfer active ester condensation: A novel technique for peptide segment coupling. *Tetrahedron Lett.* 85, 8711–8714.
- (33) Kolb, H. C., and Sharpless, K. B. (2003) The growing impact of click chemistry on drug discovery. *Drug Discovery Today.* 8, 1128–1137.
- (34) Kitov, P. I., and Bundle, D. R. (2003) On the nature of multivalency effect: a thermodynamic model. *J. Am. Chem. Soc.* 125, 16271–16284.

BC100097R